EurJOC
European Journal of Organic Chemistry

Research Article
doi.org/10.1002/ejoc.202101567

Chemistry Europe
European Chemical Societies Publishing

www.eurjoc.org

Silk–Fibroin-Supported Palladium Catalyst for Suzuki-Miyaura and Ullmann Coupling Reactions of Aryl Chlorides

Giorgio Rizzo,[a] Gianluigi Albano,[a] Teresa Sibillano,[b] Cinzia Giannini,[b] Roberta Musio,[a] Fiorenzo G. Omenetto,[c] and Gianluca M. Farinola*[a, c]

Recently, we have reported the preparation of a silk fibroin-supported Palladium catalyst (Pd/SF) and its use in the Suzuki-Miyaura cross-coupling of aryl iodides. Since its synthetic applicability and structural features are still far from being fully explored, a deeper investigation is reported here. Pd/SF is tested as a catalyst for the Suzuki-Miyaura and Ullmann coupling reactions of aryl chlorides, in H_2O/EtOH solvent mixture under atmospheric conditions. Starting from the analysis of the products of the Pd/SF promoted Ullmann reactions of poly-haloarenes, we can hypothesize the existence of catalytic pockets where monoatomic palladium species can form stable complexes with SF. To shed light on this hypothesis, Pd/SF is characterized by Wide-Angle X-ray Scattering (WAXS) analysis, which supports the supposition of catalytic pockets. Finally, using a computational model developed by Molecular Mechanic Energy Minimization we have estimated the dimension of the catalytic pocket of Pd/SF (about 15 Å), in good agreement with the experimental results.

Introduction

Silk fibroin (SF) from *Bombyx mori* cocoons is a protein biopolymer, consisting predominantly of only five α-amino acids (glycine, 45%; alanine, 30%; serine, 12%; tyrosine, 5%; valine, 1.8%) organized into hydrophobic crystalline antiparallel β-sheet domains alternated to a limited number of hydrophilic disordered regions, which instead may contain other polar α-amino acids.[1] Due to its peculiar structure, SF not only exhibits exceptional mechanical properties in terms of stiffness and strength,[2] but also offers enormous opportunities for doping, processing and functionalization.[3] Therefore, it is not surprising that SF has recently attained large interest in different applications, including biomaterials for drug delivery and tissue engineering,[4] environmentally sustainable platforms for photonic and optoelectronic devices,[5] valuable supports for metal catalysts.[6]

Bi(hetero)aryl and other related structural units represent important scaffolds in numerous natural products and many biologically active compounds.[7] Therefore, development of efficient methods for the generation of aryl–aryl bonds is a critical step to produce these compounds, and a milestone in their industrial-scale production. Pd-catalyzed Suzuki-Miyaura[8] and Ullmann[9] coupling reactions represent some of the methods of choice for the preparation of unsymmetrical and symmetrical bi(hetero)aryl scaffolds, respectively. Although most of these reactions are performed with homogeneous Pd catalysts, the increasing attention towards environmentally friendly and industrially scalable sustainable protocols has recently boosted studies towards the use of Pd species immobilized on solid supports, which are recyclable and easy to separate from the reaction mixture.[10] A consistent number of solid matrices has been successfully employed as a support for palladium catalysts, including several natural biopolymers: alginate,[11] chitosan,[12] cellulose,[13] starch,[14] pectin,[15] wool,[16] keratin,[17] collagen[18] and even degummed SF. The first silk fibroin-supported palladium catalyst (Pd/SF) was developed by Akabori *et al.* in 1956,[6a] but over the years it has been only investigated in hydrogenation reactions of alkenes, alkynes, azides and nitro groups.[19] Actually, Pd/SF structural features, as well as its potential in carbon–carbon coupling reactions of aryl halides is very far from being fully explored.

Following our interest in the development of sustainable protocols for Pd-catalyzed cross-coupling and related reactions,[20] we recently reported a convenient method for the preparation of a SF-supported palladium catalyst, which was applied for the first time in the Suzuki-Miyaura cross-coupling of aryl iodides.[21] Reactions proceed rapidly with aryl iodides and boronic acids with different stereoelectronic properties, in H_2O/EtOH mixture as solvent using low metal loading (0.38 mol%). Compared to other biopolymer-supported palladium catalysts for Suzuki-Miyaura coupling, Pd/SF showed very high recyclability (up to 25 cycles).

Aryl chlorides are very convenient substrates in organic synthesis because they are less expensive and readily available

[a] G. Rizzo, Dr. G. Albano, Dr. R. Musio, Prof. G. M. Farinola
Dipartimento di Chimica
Università degli Studi di Bari Aldo Moro
Via Edoardo Orabona 4, 70126 Bari, Italy
E-mail: gianlucamaria.farinola@uniba.it
http://www.chimica.uniba.it
[b] Dr. T. Sibillano, Dr. C. Giannini
Istituto di Cristallografia
Consiglio Nazionale delle Ricerche (IC–CNR)
Via Giovanni Amendola 122/O, Bari, 70126, Italy
[c] Prof. F. G. Omenetto, Prof. G. M. Farinola
Silklab, Department of Biomedical Engineering
Tufts University
4 Colby Street, Medford, Massachusetts 02155, USA

Supporting information for this article is available on the WWW under https://doi.org/10.1002/ejoc.202101567

Research Article
doi.org/10.1002/ejoc.202101567

compared to the corresponding aryl bromides and iodides.[22] However, the lower reactivity of the Ar–Cl bond with respect to Ar–Br and Ar–I makes quite difficult their use in palladium-catalyzed coupling chemistry. In fact, most of the reported protocols for Suzuki-Miyaura and Ullmann coupling reactions of aryl chlorides require highly efficient homogeneous palladium catalysts, involving the use of specifically designed ligands able to activate the Ar–Cl bond.[22] Therefore, the development of supported palladium catalysts which can activate aryl chlorides and open their use as substrates in Suzuki-Miyaura and Ullmann coupling reactions is highly desirable. In this regard, Pd catalysts supported on inorganic matrices,[23] synthetic organic materials,[24] and hybrid metal-organic frameworks[25] have been successfully reported, although in most cases requiring the use of toxic solvents. Among them, one of the most interesting systems is metalloenzyme-inspired polymeric imidazole Pd (MEPI–Pd) catalyst, working in H_2O with only 66 mol ppm of palladium as metal loading, although its preparation required special conditions and it is used with high temperatures (100 °C) and long reaction times (22 h).[24c] On the other hand, to the best of our knowledge only one example of Suzuki-Miyaura coupling of aryl chlorides involving a palladium catalyst supported on biopolymers (i.e., agarose) has been reported to date, although only moderate yields of the desired products were obtained working for 24 h at 100 °C.[26]

Since general synthetic applicability and structural features of our recently disclosed Pd/SF catalyst are still far from being explored, in continuation with our previous work[21] here we report a study on its application to coupling reactions involving aryl chlorides and an investigation of its structural features. In particular, we demonstrate its ability to activate the Ar–Cl bond with the development of new protocols for the Suzuki-Miyaura and Ullmann coupling reactions of aryl chlorides based on the use of Pd/SF as catalyst, performed in a sustainable solvent (i.e., water/ethanol mixture) under atmospheric conditions. To gain a deeper insight into the Pd/SF catalyst structure and mechanism of action, characterization with Wide-Angle X-ray Scattering (WAXS) analysis is performed, which provides interesting information about the nature of the interactions between the palladium and the SF.

Results and Discussion

Pd/SF was prepared according to our procedure,[21] i.e., by soaking degummed SF for 15 minutes in a boiling 6 mM aqueous solution of $PdCl_2$ to give palladium(II)-impregnated fibers (named Pd(II)–SF), which were then treated in sequence with sodium ascorbate and sodium borohydride in order to reduce them to the final catalyst.

In our previous work[21] we demonstrated the high efficiency of Pd/SF catalyst in promoting the Suzuki-Miyaura cross-coupling reactions of aryl iodides in H_2O/EtOH mixture, using very low metal loading (0.38 mol%). However, Pd/SF would become even more attractive if an analogous catalytic activity could be demonstrated in the Suzuki-Miyaura coupling of the less reactive aryl chlorides. With this purpose, we started to investigate the performance of Pd/SF in promoting the reaction of chlorobenzene (**1a**) with 4-methoxyphenylboronic acid (**2a**), chosen as a model boronic coupling partner (Table 1).

A first experiment was performed under the optimized conditions for aryl iodides developed in our previous work,[21] i.e., using a 0.38 mol% loading of palladium, K_2CO_3 as the base and a mixture H_2O/EtOH (4:1) as the solvent, for 1 h at 75 °C (Table 1, entry 1): as expected, a very low yield (< 5%) of the coupling product **3aa** was found. Only a modest improvement (yield 21%) was observed by increasing the reaction time to 6 h (Table 1, entry 2), while a decrease of the yield was found by changing the base (Table 1, entries 3–6). The H_2O/EtOH volume ratio was a critical parameter affecting the reaction outcome: the use of H_2O/EtOH (1:1) as a solvent (Table 1, entry 7) resulted in a 33% yield of **3aa**, which unfortunately dropped to 24% by further increasing the amount of EtOH to H_2O/EtOH (1:4) (Table 1, entry 8). By keeping a volume ratio of 1: 1, ethanol was replaced with other alcohols: methanol gave a yield very similar to ethanol (36%, Table 1, entry 9), while *i*-propanol resulted in very low yield of **3aa** (5%, Table 1, entry 10). We decided to use H_2O/EtOH (1:1) as the best reaction medium, increasing the palladium loading up to 3.80 mol% (Table 1, entries 11–12): this resulted in an increase of the yield up to 42%. Temperature is another important parameter: when the reaction was carried out at 100 °C, the yield of **3aa** increased to 70% (Table 1, entry 13). Under these conditions, shorter reaction times were investigated: in 3 h the Suzuki-Miyaura coupling gave again **3aa** in 70% yield (Table 1, entry 14), while a lower yield was found after 1 h (65%, Table 1, entry 15).

In this optimization study, the presence of not negligible amounts of biphenyl as a by-product of the unavoidable homo-

Table 1. Pd/SF-catalyzed Suzuki-Miyaura coupling of aryl chlorides: optimization of the reaction conditions.

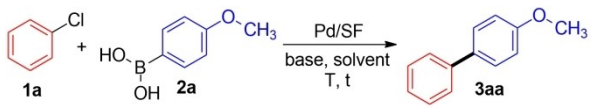

1a 2a 3aa

Entry[a]	Pd loading [mol%]	Base	Solvent	T [°C]	t [h]	Yield[b] [%]
1	0.38	K_2CO_3	H_2O/EtOH (4:1)	75	1	< 5
2	0.38	K_2CO_3	H_2O/EtOH (4:1)	75	6	21
3	0.38	NaOH	H_2O/EtOH (4:1)	75	6	23
4	0.38	K_3PO_4	H_2O/EtOH (4:1)	75	6	17
5	0.38	Cs_2CO_3	H_2O/EtOH (4:1)	75	6	13
6[c]	0.38	$NaOCH_3$	H_2O	75	6	5
7	0.38	K_2CO_3	H_2O/EtOH (1:1)	75	6	33
8	0.38	K_2CO_3	H_2O/EtOH (1:4)	75	6	24
9	0.38	K_2CO_3	H_2O/MeOH (1:1)	75	6	36
10	0.38	K_2CO_3	H_2O/*i*-PrOH (1:1)	75	6	5
11	1.52	K_2CO_3	H_2O/EtOH (1:1)	75	6	35
12	3.80	K_2CO_3	H_2O/EtOH (1:1)	75	6	42
13	3.80	K_2CO_3	H_2O/EtOH (1:1)	100	6	70
14	**3.80**	**K_2CO_3**	**H_2O/EtOH (1:1)**	**100**	**3**	**70**
15	3.80	K_2CO_3	H_2O/EtOH (1:1)	100	1	65

[a] All reactions were carried with 0.11 mmol of chlorobenzene (**1a**), 0.16 mmol of 4-methoxyphenylboronic acid (**2a**), 0.16 mmol of base, 2.5 mL of solvent, under atmospheric conditions. [b] Yields were estimated by GC-MS analysis on the crude product. [c] Reaction performed in the presence of 30 mol% of TBAB.

Research Article
doi.org/10.1002/ejoc.202101567

coupling of aryl chloride **1a** (i.e., Ullmann coupling) was always observed. Therefore, it is not surprising that in the optimized conditions (Pd loading 3.80 mol%, K_2CO_3, H_2O/EtOH 1:1 v/v, 100 °C, 3 h, Table 1, entry 14) the yield of the cross-coupling product **3aa** did not exceed 70%, despite a complete conversion of chlorobenzene **1a**.

With these optimized experimental conditions in hand, we investigated the substrate scope of the Pd/SF-catalyzed Suzuki-Miyaura coupling of aryl chlorides (Table 2). In particular, in order to confirm the synthetic applicability of the protocol, these experiments were performed on a 10 times larger scale.

First, a scale-up in the Suzuki-Miyaura reaction of chlorobenzene (**1a**) with 4-methoxyphenylboronic acid (**2a**) did not affect the yield of product **3aa** (70%). Keeping the same boronic acid **2a**, very similar yields (71–74%) were obtained with *para*- and *ortho*-chlorotoluenes **1b**–**c**. We then tested the same protocol in the coupling of aryl chlorides having different stereo-electronic properties (**1a**–**f**) with phenylboronic acid (**2b**). In the case of chlorobenzene (**1a**), Suzuki-Miyaura coupling afforded biphenyl **3ab** with an unusually high yield (99%) compared to all the other products: this result is not surprising, since in this case the unavoidable homo-coupling by-product is the same as that of the Suzuki-Miyaura cross-coupling. With all other aryl chlorides, both electron-rich and electron-poor, cross-coupling products were obtained in yields $\geq$70%, except for *p*-terphenyl **3fb** isolated in 57% yield. The protocol works quite well even by changing the stereo-electronic properties of boronic acids, although with *p*-nitrophenyl boronic acid (**2e**) 50% yield of product **3ae** was found.

The results obtained here with our Pd/SF system are definitely more convenient than those previously reported by Firouzabadi et al. for the Suzuki-Miyaura coupling of aryl chlorides catalyzed by palladium nanoparticles supported on agarose hydrogel[26] (which is, before our study, the only one example of Suzuki-Miyaura cross-coupling reactions of aryl chlorides involving a Pd catalyst supported on biopolymers): in fact, here we obtained the desired biaryl coupling products in high yields (up to 99%) after only 3 h at 100 °C, while Pd/agarose gave the cross-coupling products with lower yields after 24 h at the same temperature.

Since aryl chlorides gave no reaction under the optimized conditions for aryl iodides developed in our previous work (Table 1, entry 1),[21] this new protocol provides the valuable opportunity of sequential functionalization of iodochloroarenes by Pd/SF catalyzed Suzuki-Miyaura coupling. This possibility is exploited in the synthesis of asymmetric *p*-terphenyl **4** starting from *p*-iodochlorobenzene (**1g**) in two steps, each of them promoted by Pd/SF (Scheme 1). In the first step, **1g** was treated with phenylboronic acid (**2b**) under conditions optimized for aryl iodides (i.e., Pd/SF 0.38 mol%, K_2CO_3, H_2O/EtOH (4:1), 75 °C, 1 h),[21] affording 4-chloro-1,1′-biphenyl (**1f**) in 82% yield. In the second step, the new conditions optimized for aryl chlorides (i.e., Pd/SF 3.80 mol%, K_2CO_3, H_2O/EtOH (1:1), 100 °C, 3 h) were used in the reaction of **1f** with 4-methoxyphenylboronic acid (**2a**), to give the final asymmetric *p*-terphenyl **4** in 74% yield.

As discussed above, in our tests of Pd/SF-catalyzed Suzuki-Miyaura reactions of aryl chlorides with aryl boronic acids we always found not negligible amounts of the Ullmann homo-coupling product of aryl chlorides. Although it is often considered as an undesirable side reaction in traditional cross-coupling protocols, Ullmann coupling actually has application for the preparation of symmetrical intermediates which are present in some agrochemicals, pharmaceuticals and natural products.[9]

Starting from these results, we tested the catalytic activity of Pd/SF in the Ullmann coupling reaction: aryl chlorides **1a**–**d** were treated in the absence of arylboronic acid under similar

Table 2. Substrate scope of the Pd/SF-catalyzed Suzuki-Miyaura coupling of aryl chlorides.[a]

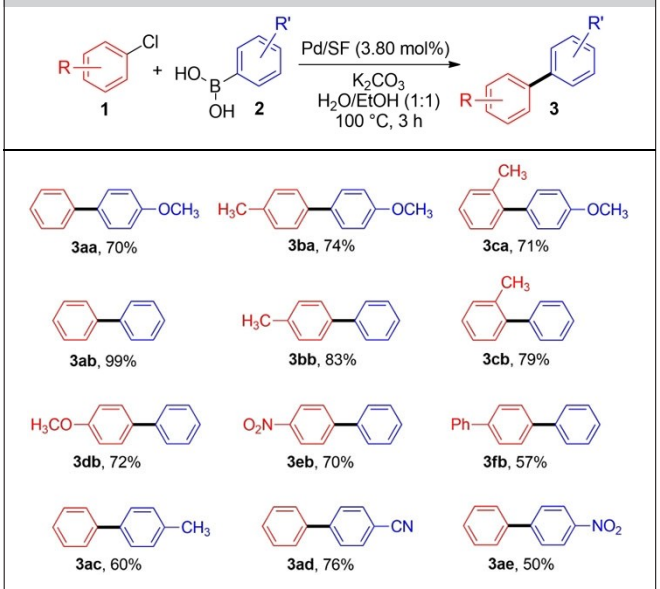

[a] Reactions were carried with 1.10 mmol of aryl chloride **1**, 1.60 mmol of arylboronic acid **2**, 1.60 mmol of K_2CO_3, 3.80 mol% of Pd/SF, 25 mL of H_2O/EtOH (1:1), at 100 °C for 3 h under atmospheric conditions. Yields of pure products after column chromatography purification are reported.

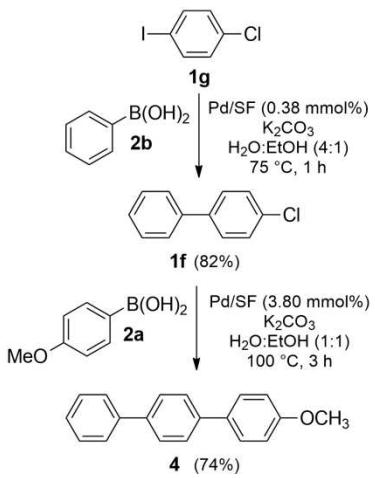

Scheme 1. Sequential functionalization of *p*-iodochlorobenzene **1g** based on our Pd/SF catalyzed Suzuki-Miyaura protocol: synthesis of asymmetric *p*-terphenyl **4** (yields of pure products after column chromatography purification are reported in parentheses).

Research Article
doi.org/10.1002/ejoc.202101567

Chemistry Europe
European Chemical Societies Publishing

reaction conditions as those used for the Suzuki-Miyaura coupling reactions: 3.80 mol% of Pd loading, 1.5 equiv. of K_2CO_3 as the base, H_2O/EtOH (1:1 v/v) as the reaction medium, at 100 °C for 4 h (Table 3). Products **5 a–d** were obtained in good yields (66–98 %), thus demonstrating a fair versatility with aryl chlorides having different stereo-electronic properties.

Table 3. Pd/SF-catalyzed Ullmann coupling of aryl chlorides.[a]

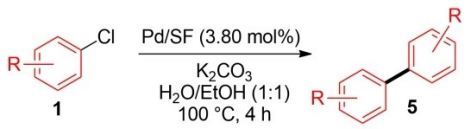

Entry	1	R	5	Ullmann product	Yield[b] [%]
1	**a**	H	**a**	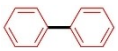	98 %
2	**b**	*p*-CH_3	**b**	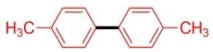	66 %
3	**c**	*o*-CH_3	**c**	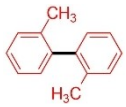	70 %
4	**d**	*p*-OCH_3	**d**	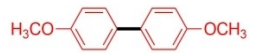	80 %

[a] Reactions were carried with 1.10 mmol of aryl chloride **1**, 1.60 mmol of K_2CO_3, 3.80 mol% of Pd/SF, 25 mL of H_2O/EtOH (1:1), at 100 °C for 4 h under atmospheric conditions. [b] Yields of pure products after column chromatography purification.

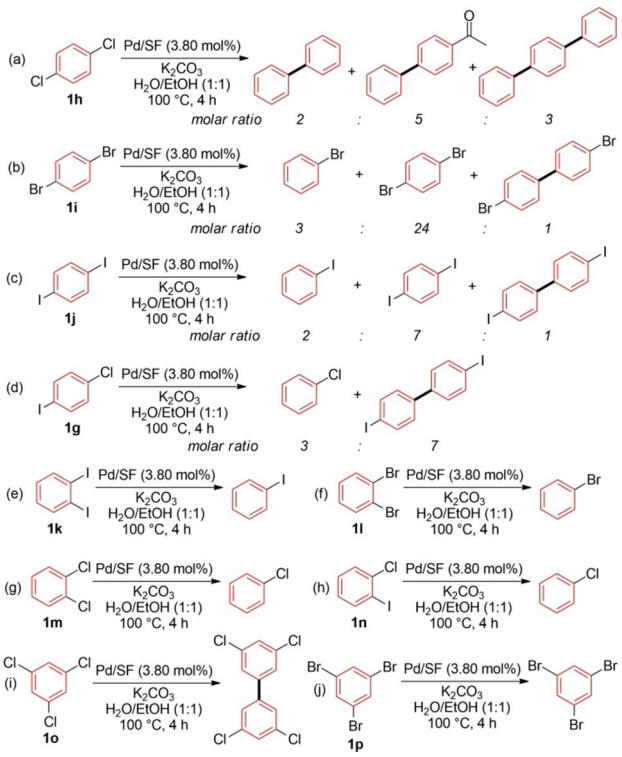

Scheme 2. Pd/SF catalysed reactions of poly-haloarenes under the optimized conditions for Ullmann coupling reactions: (a) 1,4-dichlorobenzene (**1 h**); (b) 1,4-dibromobenzene (**1 i**); (c) 1,4-diiodobenzene (**1 j**); (d) 1-chloro-4-iodobenzene (**1 g**); (e) 1,2-diiodobenzene (**1 k**); (f) 1,2-dibromobenzene (**1 l**); (g) 1,2-dichlorobenzene (**1 m**); (h) 1-chloro-2-iodobenzene (**1 n**); (i) 1,3,5-trichlorobenzene (**1 o**); (j) 1,3,5-tribromobenzene (**1 p**). For each reaction, molar ratio of the products was estimated by GC-MS analysis.

We then focused our attention on the Ullmann coupling reactions of dihaloarenes and trihaloarenes, performed under the same experimental conditions (Scheme 2). In the case of 1,4-dichlorobenzene (**1 h**), a mixture of three compounds was found in the crude product: biphenyl, *para*-terphenyl and 4-phenyl acetophenone in the molar ratio 2:3:5 (Scheme 2a). This first result proved that polymerization of **1 h** does not occur and that the maximum length of homo-coupling products is three phenyl rings, thus suggesting the existence of a size selectivity in reactions promoted by Pd/SF. The same reaction was then also tested on 1,4-dibromobenzene (**1 i**) and 1,4-diiodobenzene (**1 j**): although here we used more reactive substrates than **1 h**, in both cases the main product was the unreacted starting dihalobenzene, together with small amounts of the corresponding monohalogenobenzene and 4,4′-dihalogenobiphenyls (Scheme 2b–c). These further tests, confirming a steric dependence of substrates in Pd/SF catalyzed reactions, suggested the hypothesis of the existence of *catalytic pockets* where monoatomic Pd species could form stable complexes with suitable coordination sites on the polypeptide chains of SF. In the case of smaller 1,4-dichlorobenzene (**1 h**), able to enter inside the pocket, Ullmann homo-coupling occurred up to *para*-terphenyl products, although accompanied by dehalogenative elimination or other parasitic reactions; instead, in the case of the larger 1,4-dihalobenzene **1 i** and **1 j** any reaction hardly occurred, since they are larger than the size of pocket.

By using *p*-iodochlorobenzene (**1 g**) as the substrate, surprisingly the Ullmann homo-coupling occurred only on the chloride moieties, thus leaving the iodine atoms, despite the higher reactivity of aryl iodides compared to aryl chlorides: 4,4′-diiodobiphenyl was found as the major product, together with smaller amounts of chlorobenzene, resulting from the dehalogenative elimination of **1 g** (Scheme 2d). Then, 1,2-dihaloarenes were tested under the same conditions: 1,2-diiodobenzene (**1 k**), 1,2-dibromobenzene (**1 l**), 1,2-dichlorobenzene (**1 m**) and 1-chloro-2-iodobenzene (**1 n**). All these reactions gave the corresponding mono-halogenated benzene as the only product, with no trace of Ullmann coupling reaction (Scheme 2e–h).

Finally, we tested Pd/SF-catalyzed Ullmann coupling reactions on 1,3,5-trihaloarenes: in the case of 1,3,5-trichlorobenzene (**1 o**) we found the only Ullmann coupling product 3,3′,5,5′-tetrachloro-1,1′-biphenyl (Scheme 2i), while 1,3,5-tribromobenzene (**1 p**) gave no reaction, thus confirming the limit in the size of substrates able to interact with the catalytic pockets of Pd/SF system (Scheme 2j).

The accepted Ullmann reaction mechanism is based on a two-ways cycle, where the effective homo-coupling occurs in one case, while a dehalogenative elimination of the starting aryl halide takes place as an alternative pathway (Scheme 3).[27] The first step consists in the oxidative addition of an aryl halide molecule to the Pd species **I** to give intermediate **II**; then, deprotonation of the alcohol solvent and subsequent ligand exchange through direct Pd–O coordinative chemistry occurred, thus giving the species **III**. As a proof of this step, Ullmann reactions did not occur when only water was used as a solvent.

Research Article
doi.org/10.1002/ejoc.202101567

Chemistry Europe
European Chemical Societies Publishing

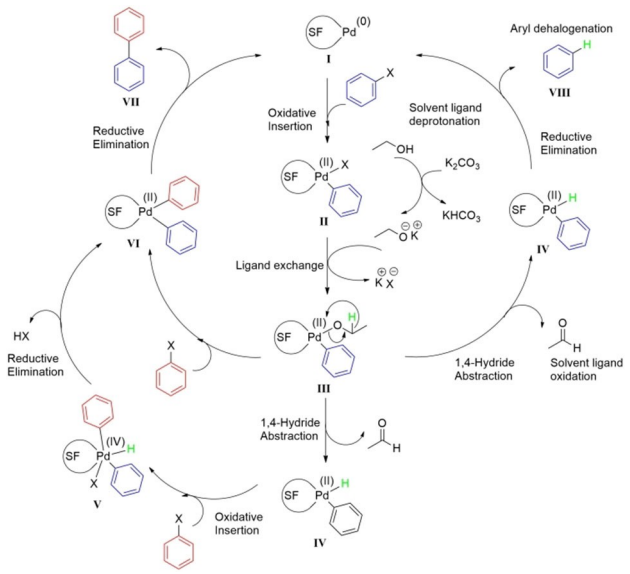

Scheme 3. Hypothetical mechanism of Pd/SF promoted Ullmann coupling reactions, according to the literature[27] and our experimental results.

Then, an oxidation of the new solvent ligand is observed, with formation of the corresponding carbonyl compounds (aldehydes from terminal alcohols, ketones for secondary alcohols) and the Palladium complex intermediate **IV**. Indeed, in our experiments we also detected acetaldehyde by GC-MS analysis as a confirmation of this oxidation process. At this point, the intermediate undergoes through the biaryl formation if another aryl halide molecule is coordinated by Pd (left pathway) or proceed with hydride migration from the oxidized solvent ligand to the aryl moiety, giving the final dehalogenative product (right pathway). As observed in our experiments, there is a strict steric control on the Ullmann coupling reactions, suggesting a confined Pd environment where only small aryl halides (1,4-dichlorobenzene **1 h**) can reasonably fit within the catalytic pocket (intermediate **V**), mimicking an enzyme-like selectivity. Bigger aryl halides (1,4-dibromobenzene **1 i** and 1,4-diiodobenzene **1 j**) instead gave the dehalogenated product, with only small traces of homo-coupling product. This hypothesis is also supported by the inverse reactivity of 1-chloro-4-iodobenzene **1 g**, where Ullmann coupling occurred only on the chloride moiety instead of the more reactive iodide. Similarly, bulky 1,2-dihalobenzenes **1 k**–**n** substrates gave only dehalogenation products. Intermediate **V**, where a Pd(IV) species is formed by oxidative insertion of a further aryl halide molecule, is reasonably the highest energy-transition state that discriminates between the two pathways in dependence of the steric hindrance of the reagents. From the maximum oxidation state of Pd in intermediate **V**, two tandem-reductive eliminations lead first to intermediate **VI** and then to the desired biaryl **VII**. Concerning the unexpected formation of 4-phenyl acetophenone product observed for 1,4-dichlorobenzene **1 h**, this is probably the product of the Palladium-catalyzed acylation of 4-chlorobiphenyl with acetaldehyde,[28] a parasitic reaction competing with the Ullmann coupling reaction. Therefore, this by-product is a further evidence of the ligand oxidation occurring the Ullmann homo-coupling reactions.

As discussed above, the analysis of the products of Pd/SF promoted Ullmann reactions of poly-haloarenes seems to suggest the hypothesis of the formation of catalytic pockets within the polypeptide SF chain, where Pd species could form stable complexes with suitable coordination sites. In order to verify this hypothesis, here we decided to perform a deeper structural investigation on Pd/SF samples.

In our previous work,[21] morphological features of Pd/SF had been investigated by Scanning Electron Microscopy (SEM) analysis, showing the absence of Pd clusters bigger than 1 nm (which is the detection limit of SEM instrument) thus suggesting that monoatomic palladium species could form stable complexes with suitable coordination sites on the polypeptide chains of SF. This result was different from what observed with other silk fibroin-supported Pd catalysts reported in literature[19b, 19c, 19e] where a dispersion of amorphous palladium metal particles on the smooth surface of SF fibers was found.

To gain more structural insights into Pd/SF catalyst structure, here we have performed WAXS investigations, which could better clarify the nature of the interactions between palladium and SF. For this purpose, degummed SF, Pd(II)–SF complex and freshly prepared Pd/SF were analyzed; we also analyzed an exhausted Pd/SF sample after 25 runs of Suzuki-Miyaura coupling, obtained in a recycling test according to our previous paper.[21]

The 2D WAXS patterns are shown in Figure 1, which display the typical cross-β fiber diffraction pattern with intensities of the main peaks distributed along two directions, the *meridional*,

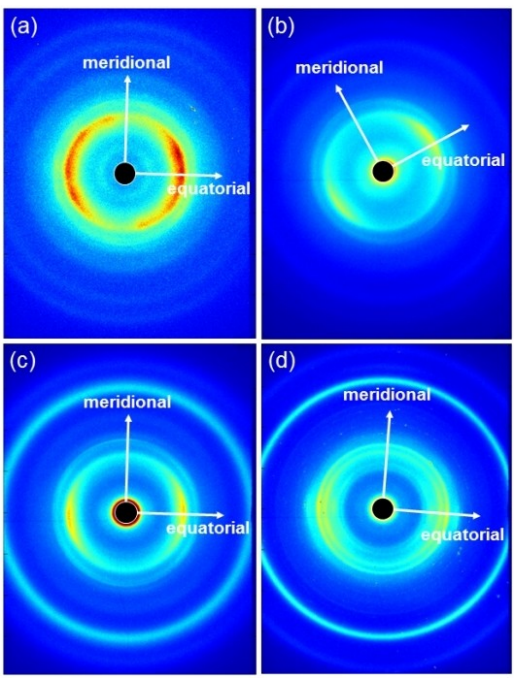

Figure 1. 2D WAXS patterns of degummed SF (a), Pd(II)–SF complex (b), freshly prepared Pd/SF (c) and exhausted Pd/SF sample after 25 runs of Suzuki-Miyaura coupling (d).

Research Article
doi.org/10.1002/ejoc.202101567

along the fiber axis, and the *equatorial*, perpendicular to the fiber axis. More in details, the meridional peaks position give information on the β strands distances along the fiber axis, whereas the equatorial peaks indicate the distance along the intersheet and interchain direction perpendicular to fiber axis. The corresponding 1D WAXS profiles are shown in Figure 2 along the two main orthogonal directions: meridional on the left column and equatorial on the right column.

The 1D WAXS profiles of degummed SF (Figures 2a–b) show all the expected peaks: the typical meridional reflection at $q = 1.79$ Å^{-1} ($d = 3.5$ Å), corresponding to the (002) planes of the crystal domain (Figure 2a, peak 1);[3c] other meridional reflections were found at 1.90 Å^{-1}($d = 3.3$ Å), 2.25 Å^{-1} ($d = 2.8$ Å), 2.81 Å^{-1} ($d = 2.36$ Å) and 3.08 Å^{-1} ($d = 2$ Å) (Figure 2a, peaks 2–5). Two further characteristic reflections were observed in the equatorial 1D WAXS profile (Figure 2b), at 1.44 Å^{-1} ($d = 4.36$ Å) and 1.70 Å^{-1} ($d = 3.7$ Å) (peaks 6 and 7, respectively).

The treatment of SF with a boiling solution of aqueous $PdCl_2$ caused its impregnation with Pd(II) ions, but this does not involve a significant variation in the 1D WAXS patterns of Pd(II)–SF (Figures 2c–d): in fact, no additional peaks relative to phase of Pd atoms are detectable, thus suggesting that Pd ions do not form any crystalline or clustering domains inside the SF structure, being hence finely dispersed in the amorphous domains of the fiber.

The following reduction into Pd/SF upon treatment with sodium ascorbate and sodium borohydride did not change any structural feature of the material: 1D WAXS patterns of Pd/SF (Figures 2e–f) appear quite similar to the previous ones, with an additional intense peak at $q = 2.81$ Å^{-1} ($d = 2.2$ Å) ascribable to the presence of crystalline domains of Pd atoms (Figure 2e, peak 8).

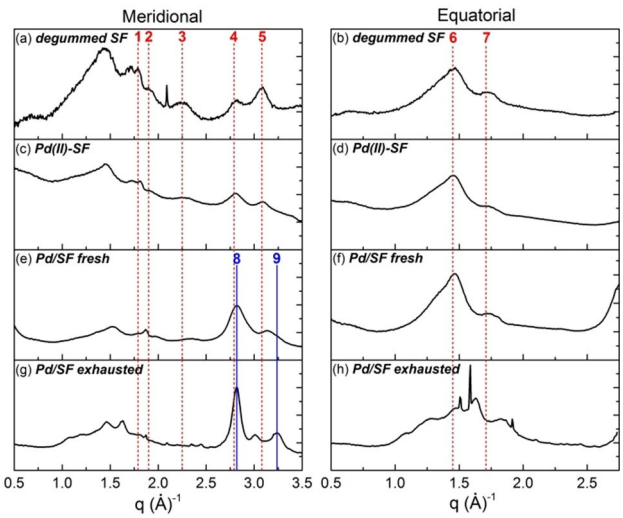

Figure 2. 1D WAXS patterns of degummed SF (a, b), Pd(II)–SF complex (c, d), freshly prepared Pd/SF (e, f) and exhausted Pd/SF sample after 25 runs of Suzuki-Miyaura coupling (g, h).along two main orthogonal directions: meridional, i.e., along the fiber axis (left column), and equatorial, i.e., perpendicular to the fiber axis (right column): For each panel, SF peaks are highlighted in red dotted lines; Pd peaks are the blue continuous lines.

Finally, WAXS investigation on the exhausted Pd/SF sample after 25 runs of Suzuki-Miyaura coupling (Figures 2g–h) showed typical reflections of the Pd cubic crystalline phase at $q = 2.81$ Å^{-1} ($d = 2.2$ Å) and $q = 3.23$ Å^{-1} ($d = 1.95$ Å) (Figure 2g, peaks 8–9), together with a shift of the peaks related to the crystalline distance along the fiber axis (peak 1 in Figure 2a shits from $q = 1.79$ Å^{-1} to $q = 1.50$ Å^{-1}) and perpendicularly to it (peak 5 in Figure 2a shifts from $q = 3.08$ Å^{-1} to $q = 3.23$ Å^{-1}). These peak shifts can be better appreciated in Figure 3, where 1D WAXS profiles of the Pd(II)–SF, fresh Pd/SF and exhausted Pd/SF are superimposed with those of the starting degummed SF. This effect can be interpreted as the result of a rearrangement of Pd atoms in crystalline clusters within SF matrix, which causes a mechanical stress of the crystalline structure of SF, increasing the distance between β-sheet crystals along the fiber axis and simultaneously compressing them in the perpendicular direction. This phenomenon could be explained by the coalescence of Pd atoms, after several catalytic cycles, generating structures that cause structural pressure inside the SF matrix. This process could also be held responsible for the loss of catalytic activity after many cycles, since palladium clustering

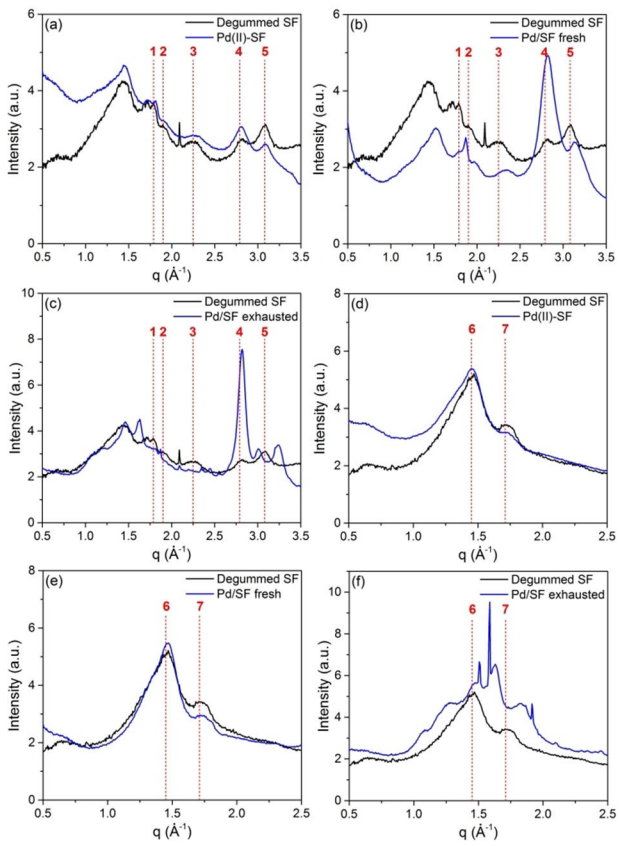

Figure 3. 1D WAXS patterns of Pd(II)–SF complex (a, d), freshly prepared Pd/SF (b, e) and exhausted Pd/SF sample after 25 runs of Suzuki-Miyaura coupling (c, f).along the meridional direction, i.e., along the fiber axis (panels a–c), and the equatorial direction, i.e., perpendicular to the fiber axis (panels d–f), in comparison with the corresponding 1D WAXS pattern of degummed SF (black curves). For each panel, SF peaks are highlighted in red dotted lines.

Research Article
doi.org/10.1002/ejoc.202101567

cause the segregation of catalytically active metal atoms, making them unable to act in cross-coupling reactions.

WAXS investigations seem to support our hypothesis of the presence of catalytic pockets in the hydrophilic disordered regions of SF, that is, specific sites where monoatomic palladium species are complexed to suitable coordination sites, probably oxygen and nitrogen atoms of the peptide bonds and oxygen atoms on tyrosine and other amino acid chains. Both reagents need to penetrate within these cavities to give the coupling reaction. To better describe this confined reaction environment, we performed some computational studies on the structure of catalytic pocket by Molecular Mechanic Energy Minimization.

As already pointed out, since WAXS analyses showed no crystalline distortion within the SF structure during both the incorporation of Pd(II) and the subsequent reduction to Pd(0) at the first catalyst preparation step, it can be reasonably assumed that the catalytic pockets and the metal atoms are predominantly located in the amorphous hydrophilic domains that connect the hydrophobic crystalline antiparallel β-sheet domains.[29] *Bombyx mori* SF is composed by a unique arrangement of Heavy Fibroin, Light Fibroin and Phybrohexamerin in a 6:6:1 cylindrical fashion. Their weights are ~350 kDa, 26 kDa and 25 kDa, respectively. Therefore, Heavy Fibroin is the main component of degummed SF. It is characterized by the alternation of twelve highly repetitive crystalline domains, formed by hexapeptides GAGAGS and GAGAGY (that constitutes over the 70% of the whole crystalline regions), linked together by eleven short amorphous and more polar regions composed by roughly 42 amino acid residues. Although the amorphous domains are non-repetitive sequences, it has been demonstrated that their variability is small and that it does not significantly change structural properties of SF.[1c] Based on these considerations and on the results already reported by Singh et al.[29], we chose as a model for computational studies a peptide constituted by 42 amino acids, i.e., GAGAGAGA-GAGTGSSGFGPYVAHGGYSGYEYAWSSESDFGTS. The optimization of the geometry of this peptide was performed by Molecular Mechanic Energy Minimization. The energy of the finally optimized geometry, obtained after 10000 iterative minimizations, was calculated at DFT (Density Functional Theory) level of approximation using the B3LYP functional. The structure of the optimized peptide is showed in Figure 4 (additional pictures are depicted in Figure S1 on Supporting Information). The total length calculated for this peptide is about 28 Å in good agreement with the value (26 Å) already reported by Singh et al.[29] Moreover, considering that the terminal edges of the amorphous regions are not easily accessible, since they are bonded to the crystalline domains, a solvent accessible surface was calculated, finding a reduced pocket entrance of about 15 Å: this is the available space of catalytic pockets, in which reagents can allocate near the coordination sphere of Palladium catalyst. Interestingly, this value is roughly comparable with the dimension of reagents used for the synthesis of biaryl products by Suzuki-Miyaura and Ullmann coupling, and perfectly fits with the analysis of the products of Pd/SF promoted Ullmann reactions of poly-haloarenes.

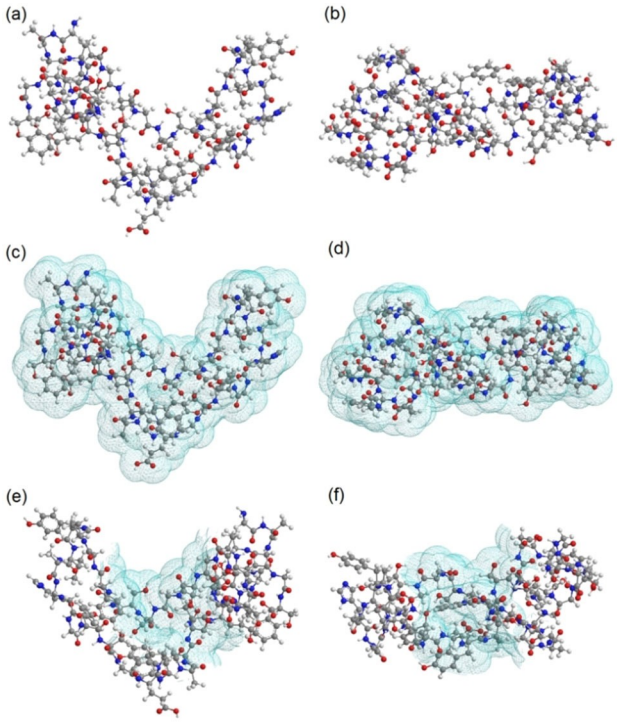

Figure 4. Different views (panels a–b) of the most stable structure in vacuo of the peptide GAGAGAGAGAGTGSSGFGPYVAHGGYSGYEYAWSSESDFGTS, selected to model the amorphous SF domains connecting the β-sheet crystals (all hydrogen atoms have been hidden). Panels c–d show the solvent accessible surface (in cyan), while in panels e–f solvent accessible surface was limited to ~15 Å, roughly corresponding to the typical dimensions of aryl halides and biphenyl products.

Conclusion

In conclusion, in the present work we have reported a deeper study on the silk fibroin-supported Pd catalyst (Pd/SF). We demonstrated the ability of Pd/SF in activating the Ar–Cl bond, whose inertia makes difficult the use of aryl chlorides in Pd-catalyzed chemistry, developing new protocols for the Suzuki-Miyaura and Ullmann coupling reactions of aryl chlorides, performed in a sustainable solvent (i.e., H_2O/EtOH solvent mixture) under atmospheric conditions. WAXS analysis afforded crucial information about the nature of the interactions between Pd and SF, supporting the hypothesis of catalytic pockets where monoatomic palladium species can form stable complexes with SF. Molecular Mechanic calculations allowed to estimate the dimension of the catalytic pocket of Pd/SF (~15 Å).

Experimental Section

General information: Degummed silk fibroin (SF) was obtained from *Bombyx mori* cocoons from Tajima Shoji (Japan) according to the procedures described previously.[3c] All the other chemicals were purchased from commercial sources and used as received without purification. Column chromatographies were performed with Fluka silica gel, pore size 60 Å, 70–230 mesh, 63–200 μm. ^{1}H-NMR and ^{13}C-NMR spectra were recorded at room temperature in

$CDCl_3$ solution with a Agilent 500 spectrometer, operating at a frequency of 500 MHz for ^1H and 125 MHz for ^{13}C, using residual solvent peak as internal reference; chemical shifts (δ) values are given in parts per million (ppm) and coupling constants (J) in Hertz. For GC-MS analyses, the GC instrument GC-TRACE-ULTRA (THERMO electron corporation) was equipped with a Fused silica capillary column OPTIMA-1-0.25 μm (30 m ×0.25 mm I.D.). Mass spectra were acquired with a POLARIS Q (THERMO electron corporation) in EI mode (70 eV).

Synthesis of Pd/SF catalyst: Degummed SF (2.10 g) was soaked for 15 min in a boiling aqueous solution of $PdCl_2$ $6\cdot10^{-3}$ M (600 mL, 3.6 mmol), then it was filtered, washed under vigorously stirring with H_2O (5×500 mL) and CH_3OH (2×500 mL) and dried under vacuum to give brown fibers. The resulting Pd(II)-impregnated SF (named Pd(II)–SF) was soaked for 24 h under stirring at 60 °C in an aqueous solution of sodium ascorbate $6\cdot10^{-2}$ M (600 mL, 36 mmol); then it was filtered, washed with H_2O (5×500 mL) and CH_3OH (2×500 mL) and dried under vacuum. After that, it was soaked again for further 10 h under stirring at 60 °C in a new $6\cdot10^{-2}$ M sodium ascorbate solution (600 mL, 36 mmol), filtered, washed with H_2O (5×500 mL) and methanol (2×500 mL) and dried under vacuum. Finally, the obtained material was soaked for 48 h under stirring at room temperature in an ethanol solution of $NaBH_4$ $6\cdot10^{-2}$ M (600 mL, 36 mmol); then it was filtered, washed with H_2O (5×500 mL) and CH_3OH (2×500 mL) and dried under vacuum to give final Pd/SF catalyst as black fibers.

General procedure for the Suzuki-Miyaura coupling of aryl chlorides (Table 2): In a 100 mL round-bottom flask, aryl chloride (1.10 mmol), aryl boronic acid (1.60 mmol), K_2CO_3 (221 mg, 1.60 mmol) were mixed into H_2O (12.5 mL) and EtOH (12.5 mL), then Pd/SF catalyst (633 mg, $4.18\cdot10^{-2}$ mmol of Pd) was added, and the resulting mixture was stirred at 100 °C for 3 h. After cooling to room temperature, the reaction mixture was diluted with H_2O and filtered through Buchner funnel. Filtrate was then extracted with *n*-hexane (3×50 mL), washed with brine (3×50 mL), dried over anhydrous Na_2SO_4 and the solvent was removed under vacuum. The crude product was purified through column chromatography on silica gel and characterized with ^1H-NMR and ^{13}C-NMR techniques.

General procedure for the Ullmann coupling of aryl chlorides (Table 3): In a 100 mL round-bottom flask, aryl chloride (1.10 mmol), K_2CO_3 (221 mg, 1.60 mmol) were mixed into H_2O (12.5 mL) and EtOH (12.5 mL), then Pd/SF catalyst (633 mg, $4.18\cdot10^{-2}$ mmol of Pd) was added, and the resulting mixture was stirred at 100 °C for 4 h. After cooling to room temperature, the reaction mixture was diluted with H_2O and filtered through Buchner funnel. Filtrate was then extracted with *n*-hexane (3×50 mL), washed with brine (3×50 mL), dried over anhydrous Na_2SO_4 and the solvent was removed under vacuum. The crude product was purified through column chromatography on silica gel and characterized with ^1H-NMR and ^{13}C-NMR techniques.

WAXS characterization: WAXS experiments were performed at the X-ray Micro Imaging Laboratory (XMI-LAB) of the Institute of Crystallography of CNR-Bari.[30] The laboratory is equipped with a Fr-E+SuperBright rotating copper anode microsource (λ= 0.154 nm, 2475 W) coupled through a focusing multilayer optics Confocal Max-Flux to a SAXS/WAXS three pinholes camera equipped for X-ray scanning microscopy. An image plate (IP) detector (250×160 mm^2, with 100 μm effective pixel size), with an off-line RAXIA reader, was employed to collect WAXS data. The spot size at the sample position was around 200 μm. The detector was placed at around 10 cm from the samples, giving access to a range of scattering vector moduli ($q=4\pi\sin\vartheta/\lambda$) from 0.3 to around 3.5 $Å^{-1}$, that correspond to 1.8–25 Å d-spacing range.

Computational details: All calculations were performed by the ChemBio3DUltra 14.0 Suite. The software is commonly used to provide optimized geometry of biopolymers and other biological structures with a scientific accuracy. According to ref [29], the 42-based amino acid peptide GAGAGAGAGTGSSGFGPYVAHGGYS-GYEYAWSSESDFGTS, (where G = glycine, A = alanine, T = threonine, S = serine, F = phenylalanine, P = proline, Y = tyrosine, V = valine, H = histidine, E = glutamic acid, W = tryptophan, D = aspartic acid) was used as a model to mime the cavity pocket where Pd atoms can coordinate to SF. The whole structure was prepared by molecular mechanic energy dynamics using a temperature increasing gradient, in order to prevent the local minimization of the peptide. Then, the model was optimized with MM2, leaving the structure to reach its absolute minimum energy after 10.000 iteration movements. The optimization procedure was performed 10 times on the same peptide structure, repeating both the MM2 dynamics and then the MM2 optimization geometry, until the optimized structure does not change anymore. Once the model was obtained, a solvent-accessible surface calculation was performed, using a 1.4 Å mean radius, corresponding to typically water-accessible surfaces.

Acknowledgements

Rocco Lassandro is acknowledged for technical support in the XMI-LAB. Open Access Funding provided by Universita degli Studi di Bari Aldo Moro within the CRUI-CARE Agreement.

Conflict of Interest

The authors declare no conflict of interest.

Data Availability Statement

Research data are not shared.

Keywords: Aryl chlorides · Palladium catalyst · Silk fibroin · Suzuki-Miyaura coupling · Ullmann coupling

[1] a) Y. Takahashi, M. Gehoh, K. Yuzuriha, *Int. J. Biol. Macromol.* **1999**, *24*, 127–138; b) C.-Z. Zhou, F. Confalonieri, N. Medina, Y. Zivanovic, C. Esnault, T. Yang, M. Jacquet, J. Janin, M. Duguet, R. Perasso, Z.-G. Li, *Nucleic Acids Res.* **2000**, *28*, 2413–2419; c) C.-Z. Zhou, F. Confalonieri, M. Jacquet, R. Perasso, Z.-G. Li, J. Janin, *Proteins* **2001**, *44*, 119–122; d) P. Cebe, B. P. Partlow, D. L. Kaplan, A. Wurm, E. Zhuravlev, C. Schick, *Acta Biomater.* **2017**, *55*, 323–332.

[2] a) T. Asakura, T. Ohata, S. Kametani, K. Okushita, K. Yazawa, Y. Nishiyama, K. Nishimura, A. Aoki, F. Suzuki, H. Kaji, A. S. Ulrich, M. P. Williamson, *Macromolecules* **2015**, *48*, 28–36; b) C. Guo, J. Zhang, J. S. Jordan, X. Wang, R. W. Henning, J. L. Yarger, *Biomacromolecules* **2018**, *19*, 906–917.

[3] a) F. G. Omenetto, D. L. Kaplan, *Science* **2010**, *329*, 528–531; b) D. N. Rockwood, R. C. Preda, T. Yücel, X. Wang, M. L. Lovett, D. L. Kaplan, *Nat. Protoc.* **2011**, *6*, 1612–1631; c) G. Rizzo, M. Lo Presti, C. Giannini, T. Sibillano, A. Milella, G. Matzeu, R. Musio, F. G. Omenetto, G. M. Farinola, *Macromol. Chem. Phys.* **2020**, *221*, 2000066; d) M. Lo Presti, G. Rizzo, G. M. Farinola, F. G. Omenetto, *Adv. Sci.* **2021**, *8*, 2004786; e) G. Rizzo, M. Lo Presti, C. Giannini, T. Sibillano, A. Milella, G. Guidetti, R. Musio, F. G. Omenetto, G. M. Farinola, *Front. Bioeng. Biotechnol.* **2021**, *9*, 653033.

[4] a) C. Vepari, D. L. Kaplan, *Prog. Polym. Sci.* **2007**, *32*, 991–1007; b) E. M. Pritchard, P. B. Dennis, F. Omenetto, R. R. Naik, D. L. Kaplan, *Biopolymers*

2012, *97*, 479–498; c) B. Kundu, R. Rajkhowa, S. C. Kundu, X. Wang, *Adv. Drug Delivery Rev.* **2013**, *65*, 457–470; d) A. B. Li, J. A. Kluge, N. A. Guziewicz, F. G. Omenetto, D. L. Kaplan, *J. Controlled Release* **2015**, *219*, 416–430; e) J. Melke, S. Midha, S. Ghosh, K. Ito, S. Hofmann, *Acta Biomater.* **2016**, *31*, 1–16.

[5] a) H. Tao, D. L. Kaplan, F. G. Omenetto, *Adv. Mater.* **2012**, *24*, 2824–2837; b) B. Zhu, H. Wang, W. R. Leow, Y. Cai, X. J. Loh, M.-Y. Han, X. Chen, *Adv. Mater.* **2016**, *28*, 4250–4265.

[6] a) S. Akabori, S. Sakurai, Y. Izumi, Y. Fujii, *Nature* **1956**, *178*, 323–324; b) I. Yoshiharu, *Bull. Chem. Soc. Jpn.* **1959**, *32*, 932–936; c) I. Yoshiharu, *Bull. Chem. Soc. Jpn.* **1959**, *32*, 936–942; d) I. Yoshiharu, *Bull. Chem. Soc. Jpn.* **1959**, *32*, 942–945; e) A. Akira, I. Yoshiharu, A. Shiro, *Bull. Chem. Soc. Jpn.* **1961**, *34*, 1067–1072; f) A. Akira, I. Yoshiharu, A. Shiro, *Bull. Chem. Soc. Jpn.* **1961**, *34*, 1302–1306; g) A. Akira, I. Yoshiharu, A. Shiro, *Bull. Chem. Soc. Jpn.* **1962**, *35*, 1706–1711.

[7] a) D. Zhang, Q. Wang, *Coord. Chem. Rev.* **2015**, *286*, 1–16; b) G. Albano, M. Morelli, L. A. Aronica, *Eur. J. Org. Chem.* **2017**, *2017*, 3473–3480; c) L. A. Aronica, G. Albano, L. Giannotti, E. Meucci, *Eur. J. Org. Chem.* **2017**, *2017*, 955–963; d) P. Devendar, R.-Y. Qu, W.-M. Kang, B. He, G.-F. Yang, *J. Agric. Food Chem.* **2018**, *66*, 8914–8934; e) G. Albano, M. Morelli, M. Lissia, L. A. Aronica, *ChemistrySelect* **2019**, *4*, 2505–2511; f) G. Albano, S. Giuntini, L. A. Aronica, *J. Org. Chem.* **2020**, *85*, 10022–10034; g) A. Punzi, F. Babudri, G. M. Farinola, *Eur. J. Org. Chem.* **2020**, *2020*, 3526–3541.

[8] a) I. Maluenda, O. Navarro, *Molecules* **2015**, *20*, 7528–7557; b) I. P. Beletskaya, F. Alonso, V. Tyurin, *Coord. Chem. Rev.* **2019**, *385*, 137–173.

[9] a) P. E. Fanta, *Chem. Rev.* **1964**, *64*, 613–632; b) F. Khan, M. Dlugosch, X. Liu, M. G. Banwell, *Acc. Chem. Res.* **2018**, *51*, 1784–1795.

[10] a) K. Köhler, R. G. Heidenreich, S. S. Soomro, S. S. Pröckl, *Adv. Synth. Catal.* **2008**, *350*, 2930–2936; b) G. Albano, S. Interlandi, C. Evangelisti, L. A. Aronica, *Catal. Lett.* **2020**, *150*, 652–659; c) G. Albano, C. Evangelisti, L. A. Aronica, *Catalysts* **2021**, *11*, 706.

[11] A. Primo, M. Liebel, F. Quignard, *Chem. Mater.* **2009**, *21*, 621–627.

[12] J. J. E. Hardy, S. Hubert, D. J. Macquarrie, A. J. Wilson, *Green Chem.* **2004**, *6*, 53–56.

[13] N. Jamwal, R. K. Sodhi, P. Gupta, S. Paul, *Int. J. Biol. Macromol.* **2011**, *49*, 930–935.

[14] V. L. Budarin, J. H. Clark, R. Luque, D. J. Macquarrie, R. J. White, *Green Chem.* **2008**, *10*, 382–387.

[15] W. Zhou, Y. Zhou, X. Zhang, B. Zeng, *Chem. J. Chin. Univ.* **2016**, *37*, 669–673.

[16] H.-c. Ma, W. Cao, Z.-k. Bao, Z.-Q. Lei, *Catal. Sci. Technol.* **2012**, *2*, 2291–2296.

[17] H. Ma, Z. Bao, G. Han, N. Yang, Y. Xu, Z. Yang, W. Cao, Y. Ma, *Chin. J. Catal.* **2013**, *34*, 578–584.

[18] Z. Dolatkhah, S. Javanshir, A. Bazgir, *J. Iran. Chem. Soc.* **2019**, *16*, 1473–1481.

[19] a) H. Sajiki, T. Ikawa, K. Hirota, *Tetrahedron Lett.* **2003**, *44*, 8437–8439; b) H. Sajiki, T. Ikawa, H. Yamada, K. Tsubouchi, K. Hirota, *Tetrahedron Lett.* **2003**, *44*, 171–174; c) T. Ikawa, H. Sajiki, K. Hirota, *Tetrahedron* **2005**, *61*, 2217–2231; d) Y. Kitamura, A. Tanaka, M. Sato, K. Oono, T. Ikawa, T. Maegawa, Y. Monguchi, H. Sajiki, *Synth. Commun.* **2007**, *37*, 4381–4388; e) H. Mirzaei, H. Eshghi, S. M. Seyedi, *Appl. Organomet. Chem.* **2019**, *33*, e5231.

[20] a) G. M. Farinola, V. Fiandanese, L. Mazzone, F. Naso, *J. Chem. Soc., Chem. Commun.* **1995**, 2523–2524; b) F. Naso, F. Babudri, G. M. Farinola, *Pure Appl. Chem.* **1999**, *71*, 1485–1492; c) F. Babudri, A. Cardone, L. Chiavarone, G. Ciccarella, G. M. Farinola, F. Naso, G. Scamarcio, *Chem. Commun.* **2001**, 1940–1941; d) F. Babudri, G. M. Farinola, L. C. Lopez, M. G. Martinelli, F. Naso, *J. Org. Chem.* **2001**, *66*, 3878–3885; e) A. Operamolla, O. H. Omar, F. Babudri, G. M. Farinola, F. Naso, *J. Org. Chem.* **2007**, *72*, 10272–10275; f) A. Operamolla, A. Punzi, G. M. Farinola, *Asian J. Org. Chem.* **2017**, *6*, 120–138; g) A. Punzi, M. A. M. Capozzi, S. Di Noja, R. Ragni, N. Zappimbulso, G. M. Farinola, *J. Org. Chem.* **2018**, *83*, 9312–9321; h) A. Punzi, N. Zappimbulso, G. M. Farinola, *Eur. J. Org. Chem.* **2020**, *2020*, 3229–3234; i) G. Albano, G. Decandia, M. A. M. Capozzi, N. Zappimbulso, A. Punzi, G. M. Farinola, *ChemSusChem* **2021**, *14*, 3391–3401.

[21] G. Rizzo, G. Albano, M. Lo Presti, A. Milella, F. G. Omenetto, G. M. Farinola, *Eur. J. Org. Chem.* **2020**, *2020*, 6992–6996.

[22] A. F. Littke, G. C. Fu, *Angew. Chem. Int. Ed.* **2002**, *41*, 4176–4211; *Angew. Chem.* **2002**, *114*, 4350–4386.

[23] a) D.-H. Lee, M. Choi, B.-W. Yu, R. Ryoo, A. Taher, S. Hossain, M.-J. Jin, *Adv. Synth. Catal.* **2009**, *351*, 2912–2920; b) M.-J. Jin, D.-H. Lee, *Angew. Chem. Int. Ed.* **2010**, *49*, 1119–1122; *Angew. Chem.* **2010**, *122*, 1137–1140; c) L. Duan, R. Fu, Z. Xiao, Q. Zhao, J.-Q. Wang, S. Chen, Y. Wan, *ACS Catal.* **2015**, *5*, 575–586; d) T. Iwai, S. Konishi, T. Miyazaki, S. Kawamorita, N. Yokokawa, H. Ohmiya, M. Sawamura, *ACS Catal.* **2015**, *5*, 7254–7264; e) S. Zhang, C. Chang, Z. Huang, Y. Ma, W. Gao, J. Li, Y. Qu, *ACS Catal.* **2015**, *5*, 6481–6488.

[24] a) D.-H. Lee, J.-H. Kim, B.-H. Jun, H. Kang, J. Park, Y.-S. Lee, *Org. Lett.* **2008**, *10*, 1609–1612; b) B. Tamami, S. Ghasemi, *J. Mol. Catal. A* **2010**, *322*, 98–105; c) Y. M. A. Yamada, S. M. Sarkar, Y. Uozumi, *J. Am. Chem. Soc.* **2012**, *134*, 3190–3198; d) B. Guo, H.-X. Li, C.-H. Zha, D. J. Young, H.-Y. Li, J.-P. Lang, *ChemSusChem* **2019**, *12*, 1421–1427; e) H. Matsumoto, Y. Hoshino, T. Iwai, M. Sawamura, Y. Miura, *ChemCatChem* **2020**, *12*, 4034–4037.

[25] B. Yuan, Y. Pan, Y. Li, B. Yin, H. Jiang, *Angew. Chem. Int. Ed.* **2010**, *49*, 4054–4058; *Angew. Chem.* **2010**, *122*, 4148–4152.

[26] H. Firouzabadi, N. Iranpoor, M. Gholinejad, F. Kazemi, *RSC Adv.* **2011**, *1*, 1013–1019.

[27] L. Shao, Y. Du, M. Zeng, X. Li, W. Shen, S. Zuo, Y. Lu, X.-M. Zhang, C. Qi, *Appl. Organomet. Chem.* **2010**, *24*, 421–425.

[28] P. Colbon, J. Ruan, M. Purdie, J. Xiao, *Org. Lett.* **2010**, *12*, 3670–3673.

[29] M. Patel, D. K. Dubey, S. P. Singh, *Mater. Sci. Eng. C* **2020**, *108*, 110414.

[30] a) D. Altamura, R. Lassandro, F. A. Vittoria, L. De Caro, D. Siliqi, M. Ladisa, C. Giannini, *J. Appl. Crystallogr.* **2012**, *45*, 869–873; b) T. Sibillano, L. De Caro, F. Scattarella, G. Scarcelli, D. Siliqi, D. Altamura, M. Liebi, M. Ladisa, O. Bunk, C. Giannini, *J. Appl. Crystallogr.* **2016**, *49*, 1231–1239; c) D. Siliqi, L. De Caro, M. Ladisa, F. Scattarella, A. Mazzone, D. Altamura, T. Sibillano, C. Giannini, *J. Appl. Crystallogr.* **2016**, *49*, 1107–1114.

Manuscript received: December 27, 2021
Revised manuscript received: December 29, 2021
Accepted manuscript online: January 3, 2022